Chinese Chemical Letters 35 (2024) 109768

Contents lists available at ScienceDirect

Chinese Chemical Letters

journal homepage: www.elsevier.com/locate/cclet

The choice of antimicrobial polymers: Hydrophilic or hydrophobic?

Zixu Xie[1], Pengfei Zhang[1], Ziyao Zhang[1], Chen Chen, Xing Wang*

State Key Laboratory of Organic-Inorganic Composites, Beijing Laboratory of Biomedical Materials, College of Life Science and Technology, Beijing University of Chemical Technology, Beijing 100029, China

ARTICLE INFO

Article history:
Received 2 January 2024
Revised 10 March 2024
Accepted 12 March 2024
Available online 16 March 2024

Keywords:
Antimicrobial polymer
Hydrophilicity
Hydrophobicity
Amphiphilicity
Chiral terpene

ABSTRACT

Owing to the spread of COVID-19, it is difficult to ignore the existence and importance of antimicrobial polymers (AMPs) because most protective appliances are made of polymers. Generally, bacteria prefer hydrophilic compounds, while fungi prefer hydrophobic ones. In recent decades, AMPs have made significant strides due to the versatile design of the functional groups or units for hydrophilic, hydrophobic, or amphiphilic performances. This review summarizes the advances of AMPs itself from the perspective of their wettability. Moreover, this study aims to clarify how the functional groups determine the interaction between the polymer and microorganisms directly affects the antimicrobial efficacy of the designed polymers. Based on the advances, the challenges and outlooks of AMPs from the perspective of wettability are systematically discussed to build a bridge between the structural design of AMPs and the requirements of practical applications.

1. Introduction

The spread of the coronavirus disease (COVID-19) has become a significant global health emergency [1–4]. The public actively seeks practical solutions to prevent the spread of disease-causing microorganisms, including viruses, bacteria, and fungi [5–8]. Numerous studies have reported that pathogenic microorganisms, especially bacteria, can remain viable and infectious on the surface of various materials for hours or even days, significantly increasing the probability of human infection [9–13]. Although conventional agents are widely used commercially to prevent microbial infections, the threat of drug resistance due to the misuse of antimicrobial agents cannot be ignored [14–20]. This phenomenon presents a significant healthcare challenge, resulting in increased morbidity, mortality, and healthcare costs. Therefore, there is an urgent need to develop new antimicrobial materials or surfaces is urgently needed as effective infection control methods to reduce the spread of pathogenic microorganisms.

Antimicrobial polymers (AMPs) are considered essential elements of antimicrobial materials or surfaces due to their controllable structures and surface properties [21,22]. The easy designability of AMPs provides an opportunity to enhance their antimicrobial performance, processability, and safety [23,24]. The research on AMPs has recently shifted from conceptual design and validation to exploring their potential for practical applications. By modifying the inherent chemical structure and surface functional groups, AMPs can be equipped with the necessary physicochemical properties and performance, such as water resistance, elongation, and desired processing properties, which can be tailored to the specific needs of different scenarios. For example, various types of AMPs have been reported, such as quaternary ammonium compounds (QACs), zwitterionic polymers, and peptide-based polymers [25–28]. These polymers have various applications in various fields, including healthcare, food packaging, water treatment, and textiles. Their antimicrobial properties are utilized to prevent infections, enhance hygiene, and extend the shelf life of products [23].

Numerous studies have reported the use of AMPs in various applications, including marine antifouling [29], household products [30], and biomedicine [31]. Wu *et al.* focused on the application of microbial polymers in the leather industry. They proposed advancements in the design strategies and synthetic methods for AMP coatings to meet the requirement of leather coating [32]. Wei *et al.* proposed a versatile method for creating AMP coatings on various substrates and discussed their representative applications in medical devices, filtration membranes, and the marine industry [33]. Luo *et al.* systematically discussed the design and platform of polymeric antimicrobial materials and outlined their applications in various fields, such as tissue engineering, personal protection, and environmental protection [34]. Borjihan *et al.* provided a comprehensive review of strategies for designing AMPs, the factors influencing their antimicrobial properties, and their applications in biomedicine [35]. In the practical applications of AMPs, different

* Corresponding author.
E-mail address: wangxing@mail.buct.edu.cn (X. Wang).
[1] These authors contributed equally to this work.

https://doi.org/10.1016/j.cclet.2024.109768
1001-8417/

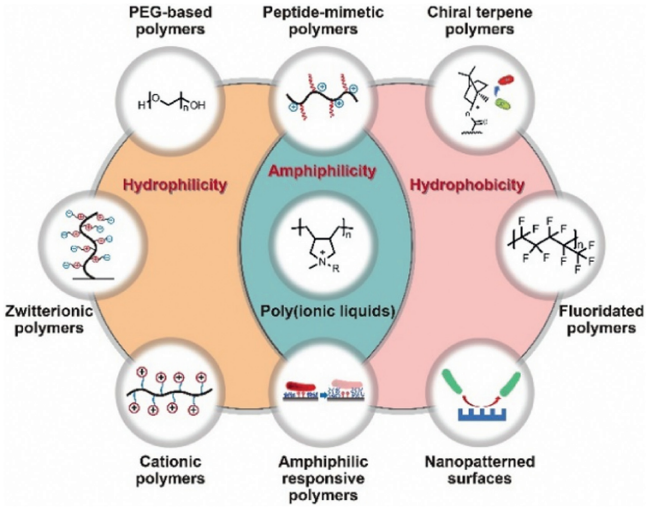

Scheme 1. Schematic of the classification of AMPs according to material hydrophilic–hydrophobic properties (hydrophilic, hydrophobic, or amphiphilic).

scenarios often necessitate different hydrophilic or hydrophobic properties on the material surface. Hydrophilic AMPs form a hydration layer through electrostatic interactions, which act as a barrier, strongly resisting bacterial adhesion. Hydrophobic materials prevent microbes from adhering owing to their inherent water-repellent nature. Microbes typically require a moist environment to attach and grow on surfaces. However, hydrophobic materials exhibit low surface energies and tend to repel water. This hydrophobicity creates a barrier that makes it difficult for water-based microbial solutions, such as bacterial biofilms, to establish a foothold on the surface. Therefore, a suitable structural design strategy must be selected for AMP materials based on the needs of the actual application scenarios. By carefully controlling the hydrophilic or hydrophobic nature of the material surface, it is possible to optimize the antimicrobial efficacy, prevent microbial attachment, and enhance the durability and performance of polymers in various applications, including medical devices, food packaging, and environmental coatings.

In this review, AMPs are classified as hydrophilic, hydrophobic, or amphiphilic based on the inherent wettability of their functional groups (Scheme 1). Representative recent studies on the development of AMPs are highlighted while excluding several topics that fall under the category of "AMPs", such as polymeric nanosystems and antibiotic-bound polymers, which can be reviewed in other literatures [35–38]. Recent advancements in various synthetic AMPs are thoroughly discussed to bridge the gap between structural design and application requirements. This will aid in guiding the on-demand design of AMPs. Furthermore, the current challenges and outlook in this field are discussed from the perspective of practical applications.

2. Hydrophilic polymer and interface

As the physicological environment is always aqueous, hydrophilic AMPs are ideal for applications involving water-based environments or biological fluids, such as biomedical implants, marine antifouling coatings, and diagnostic devices [39–42]. These AMPs include PEG-based polymers, zwitterionic polymers, and cationic polymers [43–46].

2.1. Polyethylene glycol-based polymer

Polyethylene glycol (PEG) is a long-chain polymer made up of repeated ethoxy units with varying molecular weights based on the number of ethoxy groups [47,48]. PEG is easily grafted onto the surface (a process commonly known colloquially as "PEGylation") to prevent nonspecific binding of microorganisms to the surface because the steric repulsion caused by the compression of the PEG chains and the "barrier" created by the structured water reduces bacterial adhesion on the surface [49]. Park and his colleagues investigated the bacterial adhesion behaviors on polyurethane modified with varying concentrations of PEG [50]. They discovered that the antibacterial adhesion capacity of PEG was proportional to its molecular weight, and the highest-molecular-weight PEG ($M_w = 3.4$ k) possessed an antibacterial adhesion efficiency of up to 85% within 24 h. In another study, Wang *et al.* figured out the worth of PEG coatings with different molecular weights on their resistance to the initial adhesion properties of *S. mutans* (Fig. 1A) [51]. The results revealed that the number of adherent bacteria on the PEG coating did not decrease with an increase in molecular weight, because there is generally the best molecular weight to achieve antiadhesive properties. When increasing the molecular weight of PEG from 350 to 5000, resulted in a progressive reduction in the number of adherent bacteria, culminating in a nadir at a PEG molecular weight of 5000. However, as the molecular weight increased from 5000 to 20,000, the number of adherent bacteria increased continuously. Therefore, this work showed that when preparing PEG antiadhesive coatings, a higher molecular weight of PEG does not mean a better antibacterial effect. Instead, choosing the appropriate molecular weight of PEG is important to achieve the best antiadhesive effect. To investigate the antibacterial and antifouling properties of PEG under marine conditions, Wanka *et al.* compared the resistance of a linear PEG coating (PEGMA) and a dendritic PEG coating (PGMA) to dynamic bacterial and diatom adhesion (Fig. 1B) [52]. In a dynamic marine bacterial adhesion test, the antibacterial adhesion efficiency of PEGMA (93.0%, 18 min) was significantly higher than that of PGMA (68.0%, 18 min). However, in diatom adhesion tests, the antiadhesion efficiency of PEGMA (99.0%, 20 min) was not significantly superior to that of PGMA (98.0%, 20 min). This study suggests that a more hydrophobic and less hydrated linear PEG may be advantageous for challenging coatings in marine environments.

Crosslinked network coatings of PEG have attracted significant interest. Guo *et al.* compared the antibacterial properties of two different forms of coatings using linear PEG grafting (Ti-tannic acid (TA)-PEG) and crosslinked networks (Ti-TA/PEG) [53]. The antiadhesion efficiencies of Ti-TA/PEG against *Escherichia coli* (*E. coli*) and *Staphylococcus aureus* (*S. aureus*) were 85.4% and 87.6%, respectively (Fig. 1C). By contrast, the antiadhesion efficiencies of Ti-TA-PEG against *E. coli* and *S. aureus* were 79.6% and 78.6%, respectively. Therefore, the antiadhesive properties of the crosslinked network coating of PEG were significantly stronger than those of the coating grafted with only PEG. Subsequently, Kim *et al.* investigated the potential of PDA/TA/PEG coatings for marine antifouling applications (Fig. 1D) [54]. This coating reduced the adhesion of diatoms by 83.4% within 10 days. Although this study illustrates the potential of PEG crosslinked networks in marine antifouling, it only tested the antiadhesive properties against a single algal species and lacked antifouling experiments in complex marine environments. In addition, the testing time was relatively short, which may not satisfy the demand for persistent marine antifouling materials. Han *et al.* reported antimicrobial hydrogels with different ratios of PEG to chitosan (CS) (Fig. 1E) [55]. By balancing the effects of surface wettability and surface potential, the best antibacterial performance of CS/PEG was obtained at a CS/PEG mass ratio of 0.1:1, with good early bacterial adhesion inhibition (98.8%, 5 h) and long-lasting colony inhibition (93.3%, 7 d). Therefore, the combined action of PEG and the polycationic structure should balance the positive charge and surface wettability to ensure a synergistic effect.

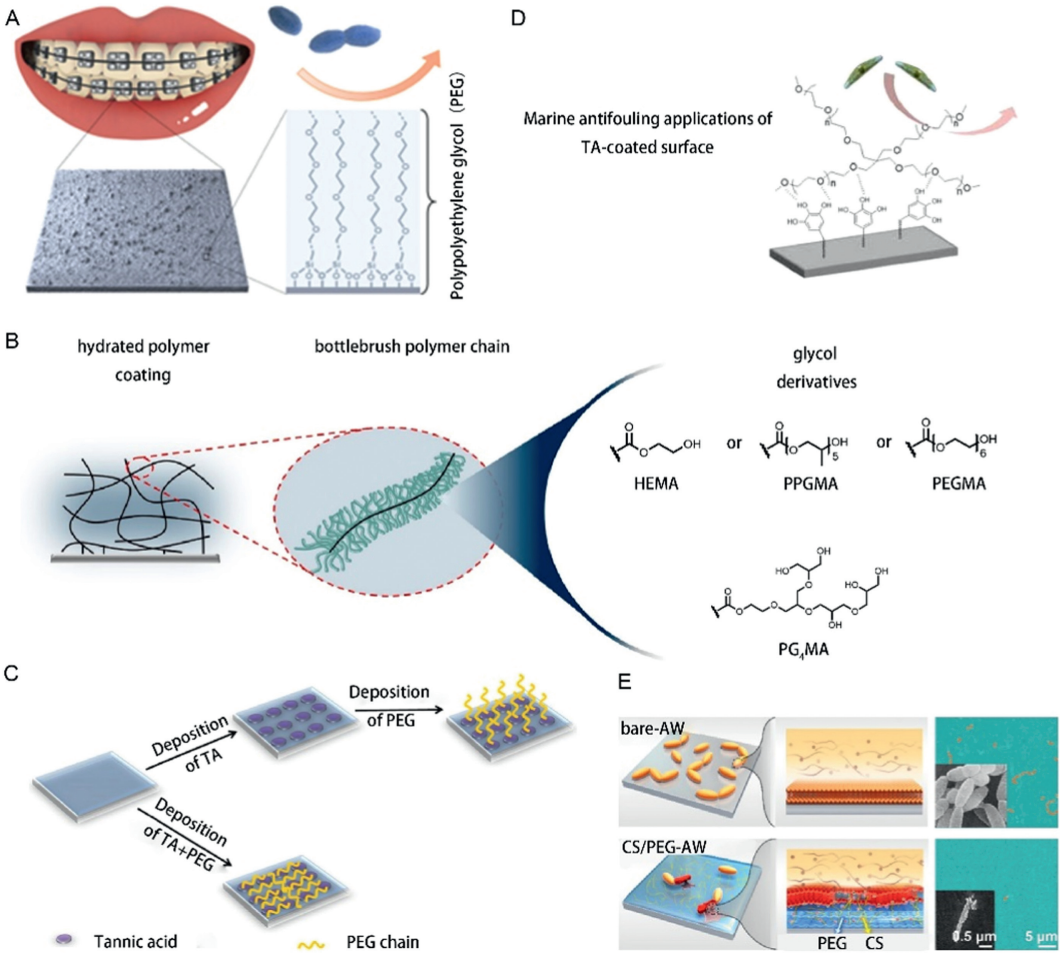

Fig. 1. (A) Long-chain PEG-coated antiadhesion orthoses. Reproduced with permission [51]. Copyright 2017, American Chemical Society. (B) Dendritic polyglycerol (PG) derivatives as marine antifouling coatings. Reproduced with permission [52]. Copyright 2021, American Chemical Society. (C) Simultaneous deposition of TA and PEG coatings on the Ti substrate surface for antifouling. Reproduced with permission [53]. Copyright 2021, Elsevier. (D) The preparation of the marine antifouling surface coating by Fe^{III}-mediated TA deposition and PEGylation. Reproduced with permission [54]. Copyright 2015, American Chemical Society. (E) Antimicrobial stainless steel with CS/PEG hydrogel coating. Reproduced with permission [55]. Copyright 2020, American Chemical Society.

2.2. Zwitterionic polymer

The use of zwitterionic polymers, which are composed of oppositely charged cationic and anionic groups on their side chains, is another strategy for the development of hydrophilic antibacterial polymers [56–59]. Compared to PEG-based coatings, whose hydration layer is maintained by weak hydrogen bonds, the hydration layer in zwitterionic polymers is more tightly bound by electrostatic interactions, making these materials more effective against bacterial adhesion [60–62].

The potential of zwitterionic polymer for antibacterial and antifouling properties has been systematically studied. Cheng *et al.* systematically investigated the biofilm resistance of zwitterionic poly(carboxyethyl methacrylate) (pCBMA) coatings under different conditions [63]. Typically, different temperatures result in differences in the long-term biofilm resistance efficiency of the pCBMA coating. At 25 °C, the pCBMA coating cleared more than 90% of *Pseudomonas aeruginosa* (*P. aeruginosa*) biofilm and could be maintained for 240 h. When the temperature increased to 30 °C, the same removal effect could last only 192 h, and only 64 h at 37 °C. Therefore, relatively low temperatures are beneficial in resisting biofilm formation. These results suggest that the biofilm resistance efficiency of coatings may depend on the experimental conditions, such as temperature, test conditions (static or dynamic), bacterial strains, and the presence of plasma.

Various zwitterionic polymer coatings have been successfully prepared to achieve hydrophilic antiadhesive modifications of material surfaces. Sundaram *et al.* developed a versatile antibacterial coating based on catechol chain-end carboxybenzene zwitterionic polymers (DOPA–PCB) (Fig. 2A) [64]. The coating showed good antibacterial adhesion efficiency (90.0%, 24 h) on several types of surfaces, including polypropylene (PP), polymethyl methacrylate (PMMA), and polyvinyl chloride (PVC). Considering the direct exposure of probacterial adhesion, PDA on the material surface may lead to a decrease in the antimicrobial capacity of the zwitterionic polymer. Kim *et al.* successfully prepared a nanometer-thick antibacterial coating using PDA, which acted as an intermediate layer of the grafted poly(sulfobetaine methacrylate) (pSBMA) (Fig. 2B) [65]. The antibacterial coating reduced bacteria adhesion by 97.0% within 6 h. Therefore, finding ways to minimize the effects of PDA on the effectiveness of antibacterial polymers is crucial when constructing antibacterial surfaces using dopamine chemistry. Click chemistry methods have also been used for the antibacterial modification of materials with zwitterionic polymers. Sae-ung *et al.* prepared a copolymer consisting of methacryloyloxyethyl phosphorylcholine (MPC) and methacrylate-substituted dihydrolipoic acid (DHLA) as structural units and formed a stable copolymer coating *via* a thiol-ene reaction [66]. The resulting poly(MPC-DHLA) formed stable coatings on various common biomedically relevant substrate surfaces, such as Si, Ti, poly(dimethylsiloxane)

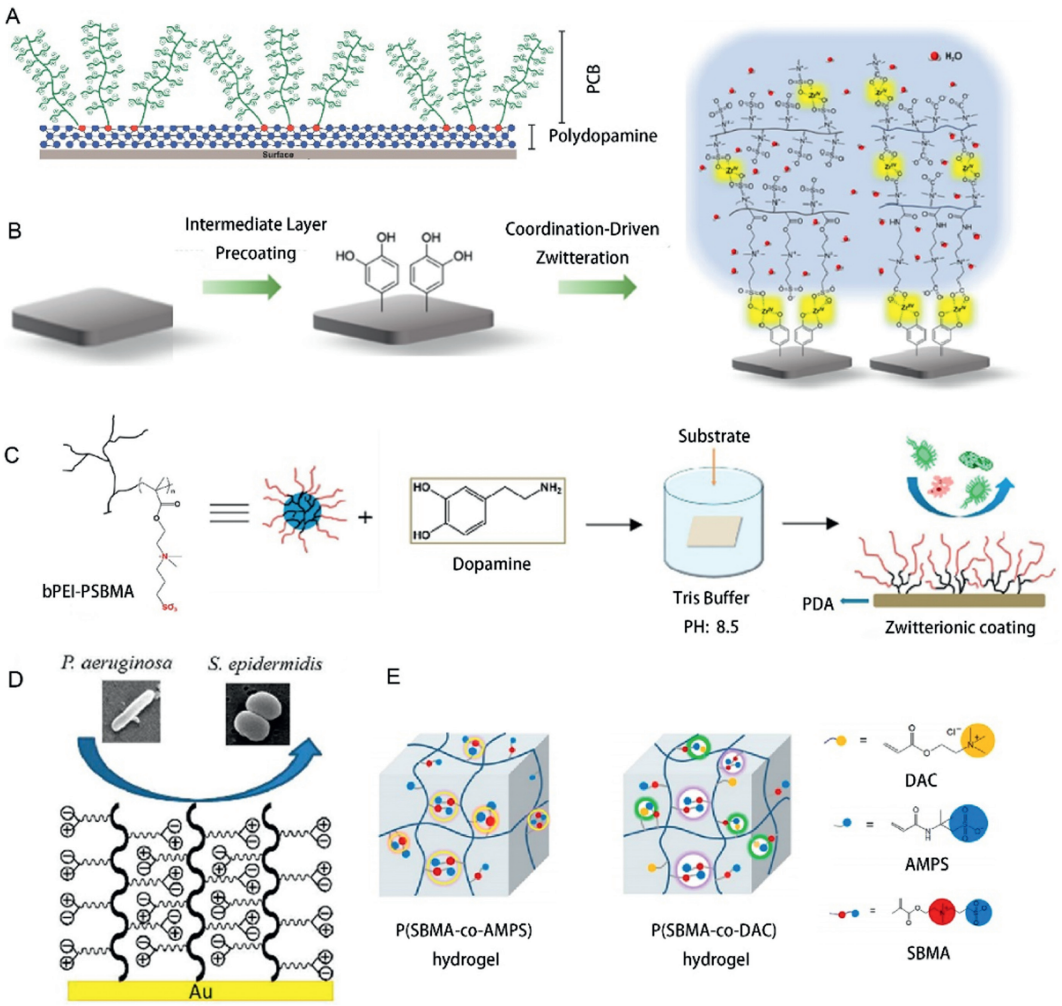

Fig. 2. (A) Mussel-inspired zwitterionic polymer brushes. Reproduced with permission [64]. Copyright 2014, Wiley-VCH. (B) Antibacterial poly zwitterionic-dopamine crosslinking coating. Reproduced with permission [65]. Copyright 2022, American Chemical Society. (C) Zwitterionic PDA/bPEI-PSBMA coatings to resist bacterial adhesion. Reproduced with permission [67]. Copyright 2018, Elsevier B.V. (D) Amino acid-based zwitterionic polymer surfaces for long-term bacterial adhesion. Reproduced with permission [68]. Copyright 2022, American Chemical Society. (E) Zwitterionic polyelectrolyte hydrogels for outstanding antibacterial properties. Reproduced with permission [69]. Copyright 2020, American Chemical Society.

(PDMS), polyethylene (PE), PMMA, and polyether ether ketone (PEEK).

Owing to the presence of MPC units in the copolymer coating, the modified surface could effectively resist biofilm formation by *S. aureus*, reducing biofilm formation by 91.0% after 1 d, 90.0% after 2 d, and 70.0% after 7 d. Integrating zwitterionic into polymers can significantly improve their antibacterial properties. Ran *et al.* prepared an antibacterial adhesion coating *via* PDA-assisted deposition of a branched polyethyleneimine-*g*-poly(sulfobetaine methacrylate) copolymer (bPEI-*g*-pSBMA) [67]. The coating showed good resistance to bacterial adhesion, reducing >95.0% adhesion within 4 h and >93.0% within 24 h (Fig. 2C). However, the authors did not study the long-term antibacterial effects of these coatings. Liu *et al.* investigated amino acid-based zwitterionic polymers (pAAZ) as surfaces or coatings that exhibited long-term resistance to bacterial adhesion (Fig. 2D) [68]. These polymers, which are derived from natural amino acids, have been found to effectively suppress bacterial adhesion. The pAAZ surfaces demonstrated remarkable resistance to bacterial adhesion even after 14 d of culture, exhibiting a reduction of at least 95% compared to unmodified surfaces. The stability of pAAZ polymers and resistance to bacterial attachment make them highly promising for applications requiring long-term suppression of bacterial adhesion. Wang *et al.* prepared an antibacterial zwitterionic hydrogel containing quaternary ammonium moieties (Fig. 2E) [69]. The abundant quaternary ammonium (QA) groups in the zwitterionic moieties and the added QA groups endow this hydrogel with an antibacterial efficiency of exceeded 99.9% within 37 h against *E. coli* and *S. aureus*. Therefore, combining zwitterionic polymers and cationic monomers or polymers can achieve both bactericidal and antiadhesive effects.

2.3. Cationic polymer

In fact, applying pure antiadhesive polymers is limited to areas where rapid sterilization is required (*e.g.*, water disinfection and food packaging). Luckily, cationic polymers have fast and efficient bactericidal properties that are effective because they interact with and adhere to negative charges on the bacterial surface, causing wrinkling and deformation of the microbial biofilm [70–74]. To date, these types of typical cationic polymers have been studied extensively in various fields.

Quaternary ammonium salt-modified polymers demonstrate efficient killing properties against pathogens [75,76]. Dong *et al.* reported the phosphonate/quaternary ammonium copolymer p(DEMMP-*co*-TMAEMA) as an anchorable antibacterial coating for metallic materials [77]. The quaternary ammonium groups in

the copolymer enhanced the bactericidal efficiency of the coatings. When the quaternary ammonium group content reached 93.7%, the obtained coatings killed 98.8% of *S. aureus* and 99.4% of *E. coli* within 8 h. The biocompatibility of this coating was not satisfactory (relative cell viability <80.0%) because of the high cytotoxicity of the quaternary ammonium component, which may be an issue to be addressed in future studies. Bai *et al.* prepared a hydrophilic antimicrobial coating by the crosslinking of polyhedral oligo-sesquioxane-poly(quaternary ammonium compound-*co*-2-aminoethyl methacrylate hydrochloride) [POSS-P(QAC-*co*-AEMA)] and poly(*N*-hydroxyethyl acrylamide-*co*-glycidyl methacrylate) [P(HEAA-*co*-GMA)] (Fig. S1A in Supporting information) [78]. By balancing the antiadhesive and cationic components, this coating achieved 99.9% and 67.2% growth inhibition of *E. coli* and *S. aureus*, respectively, within 24 h. In addition, the cytotoxicity of this coating was high, with a relative cell viability of ~25.0%. The introduction of the hydrophilic polymer component did not improve the cell survival of the quaternary-ammonium-containing coating but instead reduced its bactericidal efficiency against bacteria. Large-scale production of quaternary-ammonium-based polymers has always been a challenge. Zhang *et al.* designed a highly heat-resistant quaternary ammonium salt monomer and successfully prepared an intrinsically antibacterial polyester suitable for mass production *via* melt polycondensation [79]. This polyester exhibited fast and efficient bactericidal activity, as well as nonleaching and long-lasting antibacterial stability. The antibacterial experiments showed that the obtained polyester killed 99.9% of *E. coli* and *S. aureus* within 1 h and maintained 99.9% antibacterial efficiency after 1 m of immersion or 100 washes. This study provides a viable method for mass production of antimicrobial polyesters.

Another typical cationic polymer is the guanidinium-based polymer. Polyhexamethylene diamine guanidine (PHMG) is widely used in the water treatment, wound healing, and textile coating industries because of its efficient bactericidal activity [80,81]. Villanueva *et al.* prepared an antibacterial PVC material by grafting PHMG [82]. The obtained PVC maintained efficient bactericidal activity (99.9%, 24 h) and durable antibacterial stability (99.9%, 60 d) against *P. aeruginosa*, *S. aureus*, *Acinetobacter baumannii (A. baumannii),* and *Bacillus subtilis (B. subtilis)*. In another study, Cao *et al.* prepared PHMG-*grafted* PP (PP-*g*-PHMG) and mixed pure *p*olyethylene terephthalate (PET) and PP-*g*-PHMG in different ratios to prepare antibacterial PET materials [83]. The bactericidal efficiency of the modified PET gradually increased with increasing the PP-*g*-PHMG ratio. PET containing 3.5% PP-*g*-PHMG achieved 99.9% bactericidal activity against both *E. coli* and *S. aureus* within 24 h. Further experiments showed that the antibacterial components of this PET material were mainly enriched on the surface of the material and had nonleaching properties. The biosafety of a material is important if it is to be used as a medical device or an implantable material. Therefore, assessment of the biosafety of antibacterial polymers containing guanidine may require more in-depth studies. The degradation of guanidine-containing polymers to reduce their cytotoxicity after bactericidal effects may be feasible. In addition, *N*-halamine polymers have attracted considerable attention because of their renewable antibacterial properties and diverse molecular structures [84]. Chien *et al.* explored the effectiveness of co-deposited coatings comprising chlorinated polydopamine (PDA) and polyethyleneimine (PEI) in eradicating *S. aureus* and *E. coli*. Their findings revealed that the chlorinated co-deposition coatings exhibited significantly superior antibacterial properties in comparison to their non-chlorinated counterparts (Fig. S1B in Supporting information) [85]. Jing *et al.* first prepared amine-containing polymers (PTMPM) by polymerizing 2,2,6,6-tetramethyl-4-piperidinyl methacrylate (TMPM) and the quaternary ammonium monomer trimethyl-2-methacryloyloxyethylammonium chloride (TMAC), followed by sodium hypochlorite treatment to prepare chlorinated poly(2,2,6,6-tetramethyl-4-piperidinyl methacrylate) (Cl-PTMPM) (Fig. S1C in Supporting information) [86]. These results indicate that the antibacterial activity of Cl-PTMPM is not positively correlated with the amount of active chlorine in the polymer. The copolymer with 30% active chlorine killed >99.9% of the bacteria within 10 h, which was greater than the antimicrobial activity of the copolymers with 50% and 70% active chlorine. This is because the hydrophilic side chains of TMAC were wrapped around the hydrophobic Cl-TMPM units. When the content of Cl-TMPM increased, the hydrophobic enhancement of Cl-TMPM made contact with bacteria more difficult, and thus, the contact bactericidal effect of active chlorine could not be achieved, leading to a decrease in antibacterial activity. This work illustrates that when designing *N*-halamine polymers, the wettability of the copolymer units should be fully considered to determine the right hydrophilic-hydrophobic balance to achieve the best antibacterial activity. *N*-Halamine polymers have shown potential as bioprotective agents. Wang *et al.* fabricated a novel polysulfonamide (PSA) *N*-halamine electrospun nanofiber membrane using Lewis acid-assisted chlorination [87]. This fibrous membrane exhibited rechargeable and fast bactericidal properties and inactivated 6 log (99.9999%) of *E. coli* and *S. aureus* in 3 min. *N*-Halamine polymers have rechargeable and rapid bacterial inactivation properties and can be considered for applications such as protective masks, protective clothing, and filter membranes. Considering the requirements of these applications, their biosafety must be further evaluated.

3. Hydrophobic polymer and interface

Unlike the antimicrobial performance of hydrophilic polymers, hydrophobic polymers could directly disrupt the cell membrane or avoid the adhesion of microbes [23,88,89]. Thus, hydrophobic AMPs are used for water repellency and preventing wetting in applications such as self-cleaning coatings, food packaging, and water-repellent textiles [90–92]. Those AMPs include fluorinated polymer, chiral terpene polymer, and special nanopatterned surface.

3.1. Fluoridated polymer

The ability of fluorinated groups to impart low surface energy to polymers has led fluorinated polymers to be considered candidates for avoiding bacterial adhesion and inhibiting biofilm formation [93–97]. When bacteria and fluorinated polymers come in contact, an air layer appears between them, reducing bacterial adhesion [98,99].

The direct injection or spraying of fluorinated polymers onto a substrate surface to modify bacterial resistance is a simple but useful method. Li *et al.* injected perfluoropolyether (PFPE) lubricants onto a glass surface using a porous polybutyl methacrylate-copolymerized ethylene dimethacrylate copolymer [100]. The obtained material was able to resist the biofilm formation of 96.7% of *P. aeruginosa* within 7 d. Using the same preparation method, Xiao *et al.* investigated the potential of studying coatings formed by fluorine-inert FC-70 lubricants for marine antifouling applications [101]. This coating exhibited antiadhesion rates of 73.0% and 92.0% at 100 h for the Sporelings of *Ulva linza (U. linza)* and *Balanus amphitrite (B. amphitrite)* cyprids, respectively. Considering the complexity of marine environments, the long-term stability and environmental toxicity of such coatings should be further investigated. To enhance the antibacterial effect of fluorinated polymers, Bi *et al.* first prepared nanoscale polymer nanoparticles containing fluoroquaternary ammonium salts by emulsion copolymerization and then prepared antibacterial surfaces using a spraying method (Fig. S2A in Supporting information) [102]. The resulting films exhibited good antibacterial properties with antibacterial efficiencies

of 99.9% within 24 h. This study demonstrated that introducing a bactericidal component can significantly enhance the antibacterial properties of fluoropolymers. To investigate the effects of fluoropolymers on long-term resistance to biofilm formation, Terada *et al.* prepared a polymer coating containing tetrafluoroterephthalic acid (TFPDM) (Fig. S2B in Supporting information) [103]. This coating inhibited biofilm formation (30 d), with a 68.7% reduction in *B. subtilis* and a 93.8% reduction in *E. coli*.

In addition, grafting fluorinated polymers onto a material can achieve antibacterial modification performance. Laitman *et al.* prepared PP-poly(1*H*,1*H*-heptaflourobutyl methacrylate) (PP-PHFBM) films at room temperature *via* redox grafting polymerization (Fig. S2C in Supporting information) [104]. Compared to the PP films, PP-PHFBM was effective in biofilm formation by highly pathogenic *E. coli* and *Listeria*, with inhibition rates of 37.0% and 86.0% within 24 h, respectively. The antibacterial adhesion performance of the coating in this study was not very satisfactory, which may be related to the grafting density of the fluorinated polymers. To prepare coatings with a higher density of fluorinated functional groups, Zhu *et al.* prepared a series of copolymers containing short fluoroalkyl or perfluoropolyether and crosslinked functional groups through free radical polymerization and investigated the antibacterial performance of the copolymers as crosslinked network coatings [105]. The coatings containing perfluoropolyether chains showed an antibacterial adhesion rate of >99.0% at 24 h, indicating better antibacterial adhesion efficiency than coatings containing short perfluorinated alkyl chains. Therefore, the crosslinked network coating significantly enhanced the antibacterial performance of the fluoropolymers. In addition, when preparing fluorinated antibacterial polymers/coatings, polymers containing perfluoropolyether chains can be selected to improve antibacterial efficiency.

3.2. Chiral terpene polymer

Inspired by sensing and recognizing the surface functional groups of living organisms in nature, materials with chiral molecular structures are likely to effectively prevent microbial contamination [106,107]. Wang *et al.* found that the adhesion behavior of bacteria or fungi differed significantly for materials modified with different chiral structures of terpene molecules and were the first to propose a new antimicrobial strategy called the chiral stereochemical strategy (CCS). The chiral structure of borneol is the most representative chiral terpene molecule and significantly influences the adhesion behavior of microorganisms. Luo *et al.* successfully prepared a series of polyphenylacrylates with different chiral lobster side chains (PLBA, P DBA, and PIBA) (Fig. 3A) [108]. The three polymers showed significant differences in their adhesion behavior to bacteria, with PLBA showing a significantly higher antiadhesion efficiency than PDBA and PIBA. The anti-adhesion efficiencies of PLBA against *E. coli* and *S. aureus* were 92.4% and 85.7%, respectively (4 d). This study provides valuable insights into using chiral differences in molecular structures to achieve the antimicrobial modification of materials.

Unlike conventional antimicrobial strategies, the core of CCS is the selective recognition of chiral molecular structures by microbial systems to avoid active adhesion of microorganisms to the material surface, thus achieving antiadhesion of the material to microorganisms (Fig. 3B) [109]. Sun *et al.* prepared a series of polymethacrylates with different borneol-grafting densities (P(MMA-*co*-BA)) [110]. The antibacterial adhesion properties of P(MMA-*co*-BA) were enhanced with increasing polymeric borneol monomer content. The antibacterial efficiency of the 50% borneol polymer was the same as that of the 100% borneol polymer, with an adhesion effect of 99.7% (24 h) against *E. coli*. Notably, a visual antibacterial test model (bacterial "prison break" experiment) was proposed in this work, providing a new way of thinking for establishing visual antibacterial standards. Chiral borneol-based antibacterial coatings exhibit several potential applications. Inspired by the adhesion behavior of marine mussels, Wang *et al.* introduced acrylic borneol into a polydihydroxystyrene acrylamide-*b*-(acrylic borneol) (PDA-*b*-PBA) diblock copolymer using the traditional RAFT polymerization method (Fig. 3C) [111]. The PDA-*b*-PBA coating firmly adhered to the surfaces of various materials and exhibited good antibacterial properties, with inhibition rates of 92.7% and 81.3% for *S. aureus* and *B. subtilis*, respectively. To enhance the antimicrobial properties of sugar-containing polymer coatings, Cheng *et al.* prepared a polymer coating (PLGB) containing a sugar polymer and natural borneol [112]. Owing to the presence of natural borneol, the antiadhesion efficiencies of PLGB against *E. coli* and *S. aureus* were 88.4% and 81.3%, respectively, within 24 h. The antimold adhesion effect of the coating was equally valued. Wu *et al.* prepared a hydrophobic antibacterial coating by grafting isobutylene (IBA) side groups onto aqueous polyurethane (IWPU) (Fig. 3D) [113]. The introduction of IBA imparts a unique antibacterial effect to IWPU. The antiadhesive properties of IWPU against *E. coli* and *S. aureus* within 24 h were 89.3% and 80.4%, respectively. The hydrophobic antibacterial IWPU prepared in this study has promising applications in leather production.

In addition, chiral menthol is a potential candidate for CCS. Menthol-modified cotton textiles (P(DAM-*co*-DA)-CT) were prepared by Xu *et al. via* the oxidative copolymerization of dopamine-menthol derivatives (DAM) and dopamine (DA) (Fig. 3E) [114]. P(DAM-*co*-DA)-CT showed a broad-spectrum antimicrobial effect, with antiadhesion rates >97.5% (24 h) for bacteria (*E. coli*, *P. aeruginosa*, MRSA, and VREF) and the antiadhesion grade for fungi (*A. niger*, *A. flavus*, *M. racemosus,* and *P. chrysogenum*) was 0 (30 d). Menthol confers antiadhesive properties to CT against harmful microorganisms but does not affect the skin flora. Polymers based on chiral menthol also exhibit good antimicrobial effects. Li *et al.* prepared a series of triazine polymers with similar structures (P(MT-*alt*-ODA)), which were charged with hydrogen, ethoxy, deoxy, and menthol groups, and studied the interactions of these polymers with fungal spores [115]. The results showed that the menthol group plays a vital role in the antifungal adhesion of the polymers and can trap spores. Mechanistic studies have shown that the menthol group on the polymer inhibits fungal spores by rendering them dormant rather than killing them. This study elucidated the antimicrobial adhesion mechanism of chiral menthol-modified materials. Zhang *et al.* developed a series of methoxytriazine-modified PETs (Fig. 3F) [116–118]. These modified PETs exhibited good antiadhesive properties against both bacteria and fungi. In addition, these studies demonstrated that the antiadhesive characteristics of chiral menthol-modified polymers were caused by the stereochemical structure rather than by the wettability of the material or the bactericidal effect of menthol. These studies further advance the applications of chiral menthol in CCS.

Recently, the synergy between stereochemical polymers and other antimicrobial substances has been discovered, which enhances the antimicrobial properties of stereochemical polymers. Song *et al.* synthesized copolymers containing fluorine and borneol groups (PBAF) [119]. By adjusting the content ratios of total fluorine and borneol groups in the polymer, antiadhesion rates of >90.2% against *E. coli* and *S. aureus* were achieved. In marine antifouling tests, the polymer coating containing fluorine group/borneol groups (1:0.09) showed the best ability to resist 83.5% of mussel adhesion. Further studies have shown that borneol monomers can effectively reduce the expression of adhesion proteins in mussels. This study demonstrates the selective recognition of marine organisms by opposing terpene polymers and provides a reference method for preparing marine antifouling materials. Chen *et al.* prepared an antifungal coating by surface pho-

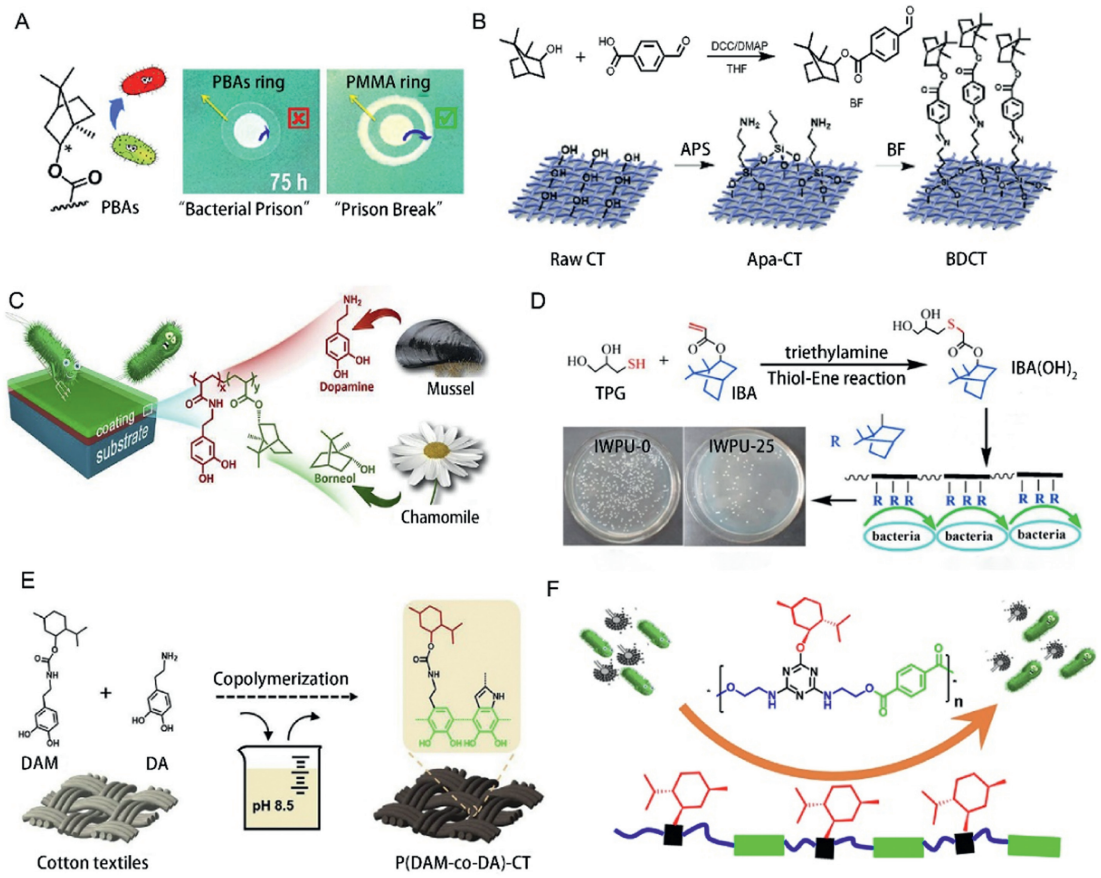

Fig. 3. (A) Evaluation model and results of antimicrobial adhesion of PBA polymer. Reproduced with permission [108]. Copyright 2014, American Chemical Society. (B) A borneol-decorated CT (BDCT) through coupling of borneol 4-formylbenzoate molecules onto the amino-modified CT is reported as microbially antiadhesive cotton. Reproduced with permission [109]. Copyright 2019, Wiley-VCH. (C) Diblock copolymer *via* RAFT polymerization of bioinspired dopamine and borneol monomers for efficient broad-spectrum antibacterial performance and robust adhesiveness. Reproduced with permission [111]. Copyright 2017, Elsevier B.V. (D) Antibacterial adhesion surfaces based on bioinspired borneol-containing glycopolymers. Reproduced with permission [113]. Copyright 2022, Royal Society of Chemistry. (E) Polyamides containing a methoxy-triazine structure. Reproduced with permission [114]. Copyright 2021, American Chemical Society. (F) Menthoxytriazine modified poly(ethylene terephthalate) for constructing an anti-adhesion surface. Reproduced with permission [117]. Copyright 2022, Elsevier B.V.

tograft polymerization using bimolecular polyethylene glycol diacrylate (PEGDA) and borneol acrylate (BA) as hydrophilic and stereochemical components, respectively [120]. The obtained coating effectively repelled ~100% of *A. niger* within 8 d by modulating the hydrophilic-stereochemical balance. The introduction of PEGEA increased the grafting density of BA, and the introduction of BA enhanced the antiadhesion ability of PEGEA to mycobacteria. Thus, combining the CCS and antiadhesion strategies is a win-win result. To address the problem that chiral terpene-modified polymers cannot kill actively adhering microorganisms, Zhang *et al.* proposed a synergistic strategy using cationic and chiral monomers to prepare a PET fabric finished with the cationic polymer PEI and chiral monomer borneol (Fig. 4) [121]. The obtained fabrics exhibited high bactericidal efficiencies (93.5% for *E. coli* and 99.1% for *S. aureus*) and good antimold adhesion efficiencies (99.9% for *A. niger* and *M. racemosus*). The introduction of chiral borneol not only effectively compensated for the lack of antifungal ability of PEI but also reduced the cytotoxicity of PEI. In the future, the combined action of stereochemical and traditional bactericidal components (such as quaternary ammonium salts and nanoparticles) will be a new direction for developing CCS.

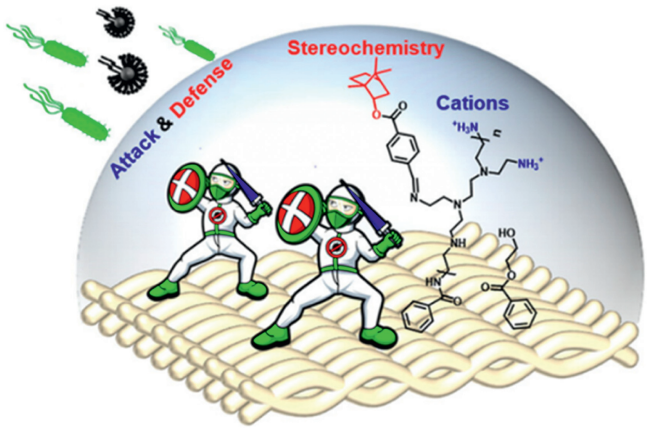

Fig. 4. Dual coordination between stereochemistry and cations endows polyethylene terephthalate fabrics with diversiform antimicrobial abilities. Reproduced with permission [121]. Copyright 2023, American Chemical Society.

3.3. Hydrophobic nanopatterned surface

The aforementioned studies discussed changes in material hydrophilicity or hydrophobicity upon incorporating functional groups, thereby enhancing the antimicrobial properties of the materials. In addition, nanopatterning can further modify the surface morphology and topological structure of the materials. Particularly, nanopatterning allows the creation of microscale structures, such as nanoparticles, nanowires, and nanopores, on the surface of a

material, thereby influencing its surface morphology, roughness, hydrophobicity, and other characteristics [122–124].

Inspired by the layered structure of natural materials, engineered surfaces with specific micron and/or nanomorphologies also offer a way to combat biological contamination [125–127]. Nanopatterned surfaces endow good antibacterial properties to materials by mimicking the morphological characteristics of natural surfaces [128–131]. The construction of material surfaces at the nanometer or micron-scale by nano-patterning is effective in reducing bacterial adhesion and killing bacteria (Fig. S3A in Supporting information) [132–134]. Nanopatterned polymers exhibit antiadhesive or physical bactericidal effects on pathogens, depending on their surface morphology [135].

The most typical nanopatterned surface model is a shark skin-inspired material. The shark's unique skin structure hinders the formation of biofilms by different mechanisms, such as reducing attachment sites, generating turbulence, promoting self-cleaning, and potentially possessing antibacterial ability. The study has shown that the surface of this type of material has increased roughness owing to the presence of regularly arranged ridged platelet structures, which reduce bacterial adhesion on its surface [133]. Chung *et al.* prepared a polydimethylsiloxane elastomer that mimicked shark skin micromorphology (Sharklet^{TM} PDMS) [136]. Sharklet^{TM} PDMS effectively prevented bacterial adhesion and impeded biofilm formation by *S. aureus* for 21 d (87.0% reduction) through its micromorphology rather than as an antibacterial agent. Reddy *et al.* investigated the anti-biofilm formation effect of sharklet-patterned modified Foley catheters to explore the potential of this modification scheme in the field of medical catheters. The antiadhesion efficiency of the Sharklet-modified Foley catheter against *E. coli* was 81.0% within 24 h compared with that of the smooth catheter [137]. To understand the antibacterial mechanism of sharkskin micropatterns, Chien *et al.* investigated the effect of sharkskin micropatterns with different roughness levels on bacterial adhesion and biofilm formation (Fig. S3B in Supporting information) [138]. The results showed that mature biofilms could develop on the smooth surfaces after 14 days, while extremely low levels of *E. coli* were observed on the shark skin-patterned surface because of the increased roughness. Meanwhile, another study has shown that bacterial adhesion increases with surface roughness because rough surfaces have a greater surface area and the depressions present in rough surfaces provide more favorable sites for colonization [139]. These special surface structures thwart the proliferation of microcolonies formed by diminutive bacterial clusters nestled within the recesses and disrupt the process of quorum sensing [140]. Therefore, when preparing shark skin micropatterned surfaces, different roughness levels should be selected according to the application requirements.

In addition, inspired by the ability of natural superhydrophobic surfaces, such as cicadas and dragonfly wings, to kill bacteria physically, various types of biomimetic nanopillar/spike surfaces have been widely reported. Denver *et al.* prepared nanopillar arrays on acrylic polymer films by nanoimprint lithography (Fig. S3C in Supporting information) [141]. The results showed that increasing the nanopillar spacing led to a gradual decrease in the antibacterial properties of the surfaces. Nanostructured films consisting of nanopillars with a height of 60 nm and a spacing of 30 nm exhibited significant bactericidal activity against *P. aeruginosa* (80.0%, 18 h) and *S. aureus* (90.0%, 18 h). Tripathy *et al.* fabricated nanostructured surfaces (NSS-CHI) with high aspect ratios on chitosan (Chi) surfaces using one-step deep reactive ion etching (DRIE) (Fig. S3D in Supporting information) [142]. Compared with Si, Si-CHI, and NSS, *E. coli* on the surface of NSS-CHI was reduced by 25.0%, 9.0%, and 1.0%, respectively, and *S. aureus* on its surface was reduced by 38.0%, 16.0%, and 10.0%, respectively. The authors noted that the CHI coating of NSS-CHI captured *S. aureus* between the nanostructures, followed by killing the bacteria by the nanostructures, thus improving the antibacterial efficiency. Inspired by this study, Carballal *et al.* reported nanopatterned surfaces produced by the self-assembly of block copolymers [143]. They first coated polystyrene-*block*-poly(2-vinylpyridine) (PS-*b*-P2VP) into films and then produced different nanomorphologies by solvent vapor annealing. This material killed ~99.9% of adherent *E. coli* within 30 min. The authors suggested that the hydrophilic interaction between the hydrophilic structural domain of P2VP and the lipopolysaccharide of the cell wall of *E. coli* led to a closer interaction between *E. coli* and the nanopatterned surface compared to the hydrophobic PS nanopatterned surface, which in turn promoted membrane disruption in *E. coli* and thus enhanced bactericidal activity. Therefore, the antibacterial efficiency of nanopatterned surfaces can be improved by facilitating contact between the bacteria and nanopillars.

4. Amphiphilic polymer and interface

Either hydrophilic or hydrophobic AMPs possess their intrinsic properties and suitable application scenarios. However, the microbial environment is always a multi-component and complicated system, which means that antimicrobial polymers with multi-functionalities should be addressed. Ampliphilic polymers efficiently improve their bioactivity through tuning of the hydrophobic/hydrophilic balance [144–147]. Those AMPs include peptide-mimetic polymers, poly(ionic liquids), and amphiphilic responsive polymers [24,148–153].

4.1. Peptide-mimetic polymer

Inspired by the structure of antimicrobial peptides, peptidomimetic polymers containing hydrophilic cationic and hydrophobic groups are considered efficient antimicrobial materials [154,155]. The cationic portion of the peptide-mimetic polymer drives the selective binding of the polymer to the bacterial membrane, whereas the hydrophobic portion disrupts the bacterial membrane, thus triggering bacterial death [150,156]. Several studies have shown that peptide-mimetic polymers in the drug form exhibit good antibacterial properties (Fig. 5A) [157,158]. Recently, peptide-mimetic polymers have gained attention owing to their efficient antimicrobial effects on surfaces.

To investigate the antibacterial effect and mechanism of peptide-mimetic polymer tethering on bacteria after retention on the surface, Qian *et al.* prepared a host defense peptide mimetic β-peptide polymer modified surface (Fig. 5B) [159]. The obtained surface exhibited efficient bactericidal properties, killing 99.9% of *E. coli* and MRSA within 2.5 h. Unlike the antibacterial principle of peptidomimetic polymers in solution form, immobilized peptidomimetic polymers led to the rupture of bacterial membranes by depleting the cell membrane of stable Ca^{2+} and Mg^{2+}. This study illustrated the feasibility of the antibacterial surface modification of peptide-mimetic polymers. Gao *et al.* prepared an L-lysine (K)-L-phenylalanine (F) copolymer containing a catechol moiety and deposited it on the surface of a medical catheter (Fig. 5C) [160]. The modified catheter showed >99.0% antibacterial activity against MRSA and *P. aeruginosa*. In addition, the antibacterial catheter exhibited good biofilm formation and protein/platelet resistance.

Because of the presence of cationic polypeptides (cPep) and mixed-charge polypeptides (mPep) in the polymer coating, this coating achieved a dual role of antibacterial and anti-adhesive. The authors suggested that the bactericidal mechanism of the coating was similar to that of the peptide-mimetic polymer in solution; however, no further evidence was provided. Lu *et al.* prepared

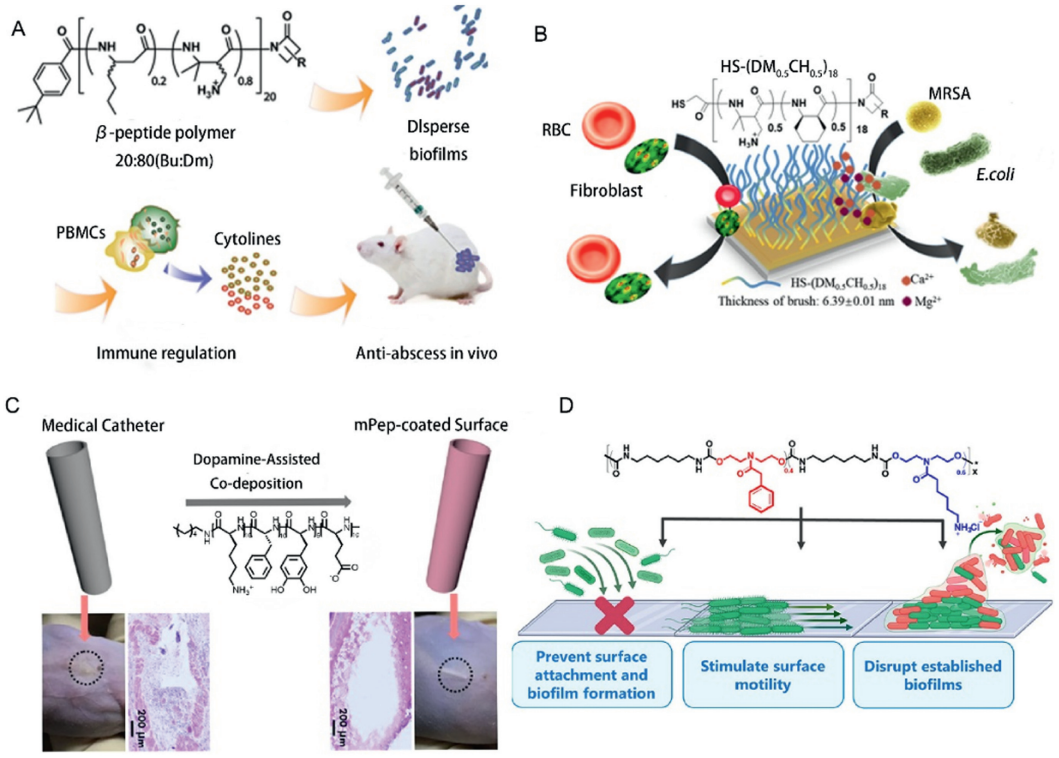

Fig. 5. (A) Preparation of antimicrobial β-peptide polymers and polymer-modified surfaces. Reproduced with permission [157]. Copyright 2018, American Chemical Society. (B) Mussel-inspired cationic polypeptide (cPep) and mixed-charge polypeptide (mPep) for enhanced hemocompatibility and anti-infective effect. Reproduced with permission [160]. Copyright 2019, American Chemical Society. (C) Surface modification of peptide polymer 90:10 DLL:BLG to enable material surfaces antibacterial properties. Reproduced with permission [162]. Copyright 2021, Elsevier B.V. (D) Schematic diagram of peptidomimetic polyurethanes inhibit and disrupt the bacterial biofilm. Reproduced with permission [162]. Copyright 2021, American Chemical Society.

a series of peptide polymer libraries and achieved the antibacterial modification of polyurethane materials (TPU) with peptide polymers for optimal antimicrobial effects using a high-throughput screening method [161]. The modified TPU rapidly killed various types of common harmful and drug-resistant bacteria within 2.5 h. it demonstrated that contact with the modified TPU resulted in a significant increase in the permeability of the outer membrane of the bacteria, along with a release of cytoplasm. Thus, this peptidomimetic polymer-modified surface killed the bacteria by disrupting their membranes. Some peptidomimetic polymers with weak antibacterial activity can also be used to achieve the antibacterial modification of materials. Vishwakarma *et al.* designed a peptidomimetic polyurethane in which an arginine mimetic group moiety was used as its cationic group, and a phenylalanine mimetic was used as a side group to regulate hydrophobicity (Fig. 5D) [162]. The resulting polyurethane-modified surface inhibited bacterial biofilm formation in the flowable medium for up to 7 d. The obtained antibacterial polyurethane modulated bacterial adhesion behavior by affecting bacterial motility rather than bactericidal action. The use of interactions between the bacteria and polymer chemical functional groups to avoid bacterial biofilm formation was similar to that mentioned earlier.

4.2. Poly(ionic liquids)

Poly(ionic liquids) (PILs) have attracted considerable attention in materials science because of their versatility and selectivity for polymer segments. From a chemical structure perspective, PILs are amphiphilic polymers typically consisting of a repeating unit consisting of a positively charged ionic liquid (IL) component and a hydrophobic alkyl chain component [152,153]. The bactericidal mechanism of PILs is similar to that of solubilized peptidomimetic polymers, both of which result from electrostatic interactions. The positively charged ILs component causes the polymer to localize in the negatively charged region of the microbial cell membrane/wall and the hydrophobic side chains to be inserted into the membrane, leading to microbial death [163].

To develop polymeric films with intrinsic antibacterial activity (without surface coating), Guo *et al.* prepared an imidazole-based PIL film by *in situ* photocrosslinking polymerization using two different amino acids (L-proline (Pro) and L-tryptophan (Trp)) (Fig. 6A) [164]. The films with 35% PIL showed the best antibacterial efficiency against *E. coli* and *S. aureus*, with a 98% inactivation rate within 4 h. However, the antibacterial activity of the polymer and PIL content were not positively correlated. The authors concluded that a high PIL content (45%) increased the hydrophilicity and induced the aggregation of the hydrophobic segments of the polymer, which prevented polymer insertion into the hydrophobic region of the bacterial lipid membrane, resulting in reduced antimicrobial activity. This study provides a valuable reference for the structural design of antibacterial PILs. To investigate the effect of hydrophobic alkyl chain length on the antibacterial efficiency of PIL membranes, Qin *et al.* synthesized a series of PILs antibacterial membranes with different alkyl chain lengths using pyrrolidine-based IL and PIL homopolymers for comparison (Fig. 6B) [165].

The antibacterial performance of both PIL homopolymers and small molecule ILs increased with the increase of the alkyl chain length of substitutions. However, the antibacterial activity of the PIL membranes decreased with increasing alkyl chain length. The author explained that when bacterial suspensions were in contact with the PIL membrane surface, pyrrolidine cations tended to diffuse into the water/polymer interface, whereas hydrophobic alkyl chains tended to be inserted into the membrane body, thus failing to achieve a better membrane-breaking effect on bacteria and

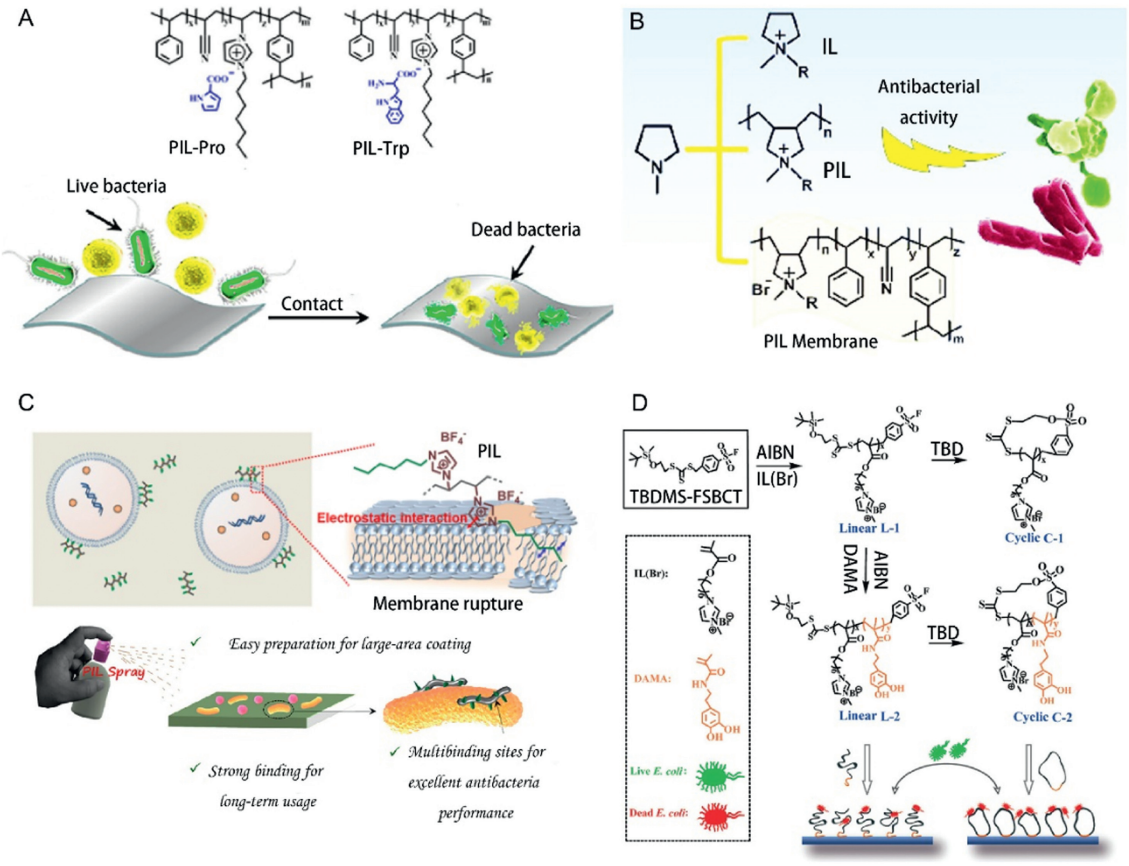

Fig. 6. (A) Robust PIL membranes with high antibacterial activities. Reproduced with permission [164]. Copyright 2015 American Chemical Society. (B) Pyrrolidinium-type PIL membranes for antibacterial applications. Reproduced with permission [165]. Copyright 2017 American Chemical Society. (C) Poly(ionic liquid) (PIL-Cn)-based efficient and robust antiseptic spray that exhibits long-term antibacterial properties. Reproduced with permission [166]. Copyright 2021 American Chemical Society. (D) Cyclic PIL brushes for enhancing bactericidal activity. Reproduced with permission [167]. Copyright 2019 Wiley-VCH.

reducing their antibacterial efficiency. However, this rule may not apply to the direct contact between PILs films and airborne bacteria and may require further in-depth study. Liu *et al.* reported a highly effective antibacterial spray based on PILs (PIL-Cn), which achieved antibacterial modification of various surfaces by simple spraying and killed 99.9% of the bacteria within 60 d (Fig. 6C) [166]. This study also found that long-chain PILs spray coatings exhibit long-term antibacterial activity (both Gram-positive and Gram-negative bacteria) on diverse substrates (glass, PE, and cotton). Furthermore, PIL agent with longer side alkyl groups shows better antibacterial performance because the longer side chains can effectively destroy the bacterial membranes through stronger hydrophobic interactions. The surface of the material grafted with the PIL brush also exhibited good antibacterial activity. Liu *et al.* prepared an antibacterial surface based on cyclic PIL brushes to investigate the effect of the topology on the antibacterial properties of the material (Fig. 6D) [167]. They compared the differences in antibacterial activity between the ring PIL structure and the corresponding linear PIL structure. The ring structure endowed the PILs with stronger bactericidal activity, with 98.3% against *E. coli* compared to 93.4% for the corresponding linear PILs brush. The enhanced antibacterial properties may be owing to the higher surface roughness and denser surface charge of the topologically structured PIL brush-modified material.

4.3. Amphiphilic responsive polymer

Considering that the accumulation of dead bacteria on antimicrobial surfaces can trigger inflammation, scientists have proposed several smart reactive polymer surfaces that respond more effectively to changes in various environmental stimuli [168–170]. These polymers kill bacteria adhering to their surfaces and release dead bacteria and other debris as needed, displaying a clean surface under appropriate stimulation and thus maintaining effective long-term antimicrobial activity [148,171–174]. In terms of material wettability, this process usually involves a conversion between hydrophilic and hydrophobic forms.

Bacterially infected sites often show a decrease in pH. Therefore, using materials that respond to different pH values to kill and release bacteria is viable. For example, Lu *et al.* prepared an amphiphilic self-defense antibacterial hydrogel coating ($PaAA_{LbL}s$) triggered by pH [175]. This hydrogel coating reduced bacterial adhesion by 99.9% within 24 h. At pH 7.4, the hydrogel with hydrophilic properties exhibited an antiadhesive effect on the bacteria. As the bacterial proliferation environment became more acidic, a hydrophobic transition of the coating was induced, and the hydrophobic segments in the polymer network were inserted into the bacterial wall, leading to wall damage and bacterial death. The authors suggested that this phenomenon was caused by the pH drop driving the conformation of the polyacid chains from coils to blobs, which allowed more hydrophobic fragments to be exposed and then inserted into the bacterial membrane, eventually leading to bacterial death. Unfortunately, this study did not investigate the antibacterial properties of the material over a longer period. Moreover, introducing bactericidal polymer seems to enhance the antibacterial properties of the material. This idea was realized by Yan *et al.* and Xu *et al.* They prepared a pH-responsive coating with poly(methacrylic acid) (PMAA) and AMP as the

inner and outer layers, respectively (Fig. S4A in Supporting information) [176]. The hydrated PMAA layer resisted the initial bacterial attachment. When bacteria colonize the surface, the acidification triggered by the bacteria exposes the bactericidal AMP, which kills ~99.9% of the bacteria within 7 h. In addition, if the environmental pH increases, dead bacteria are released once the PMAA chain regains its hydrophilicity. Applying the same idea, Xu *et al.* grafted poly(2-diisopropylaminoethyl methacrylate)-*b*-poly(2-methacryloyloxyethyl phosphorylcholine) (PDPA-*b*-PMPC) and cationic poly(lysine) (PLYS) onto a material surface (PLYS-TA-PDPA-*b*-PMPC) (Fig. S4B in Supporting information) [177]. Owing to the efficient bactericidal properties of PLYS, PLYS-TA-PDPA-*b*-PMPC exhibited significant antibacterial activity. The antibacterial results showed a 78.0% decrease in the percentage of bacteria adhering to the PLYS-TA-PDPA-*b*-PMPC coating, with 77.0% of dead bacteria. In addition, the PLYS-TA-PDPA-*b*-PMPC coating had a self-cleaning effect on the material surface because of the external pH change.

Temperature change is a universal phenomenon and therefore holds promise as an external stimulus for designing smart-responsive antibacterial materials. Yu *et al.* prepared a temperature-responsive bactericide release surface by integrating QAS into a poly(*N*-isopropylacrylamide) (PNIPAAm)-modified surface (Fig. S4C in Supporting information) [178]. PNIPAAm is a highly thermally responsive polymer. When the temperature is below 37 °C, the intermolecular H-bonds between PNIPAAm chains and water molecules dominate, resulting in a stretchy brush-like structure showing hydrophilicity. Above 37 °C, the intramolecular H-bonds in the PNIPAAm chains led to dense and collapsed hydrophobic conformations. This surface achieved efficient bactericidal activity and accumulation at 37 °C, followed by the release of dead bacteria in water below 37 °C. This strategy kills and releases bacteria in a controlled manner, enabling better long-term antibacterial resistance. Then, Yu *et al.* combined the antibacterial activity of lysozymes with the thermal responsiveness of PNIPAAm to prepare smart antibacterial surfaces [179]. When the temperature was higher than 37 °C, PNIPAAm collapsed and was dehydrated to expose the hidden lysozyme and kill the bacteria. When the temperature was lower than 37 °C, PNIPAAm was hydrated, thereby releasing the adherent bacteria. In the future, developing various types of PNIPAAm/antibacterial surfaces may become a research trend. Salt-responsive antibacterial materials have recently attracted considerable attention. Fu *et al.* combined triclosan (TCS) and poly(3-(dimethyl(4-vinylbenzyl)ammonia)propyl sulfonate) (polyDVBAPS) to develop a new "kill-release" antibacterial polymer surface (polyDVBAPS) (Fig. S4D in Supporting information) [180]. TCS rapidly kills the bacteria upon contact with normal water. PolyDVBAPS brushes have a higher stretched conformation and hydration state in salt solutions, enabling the release of dead bacteria, a process that also involves hydrophobic-to-hydrophilic conversion. The surface exhibited high bactericidal activity against *E. coli* and *S. aureus* within 2 h (>95.0%). In addition, 97.0% of the attached bacteria were released in highly concentrated salt solutions (>0.53 mol/L) owing to their isolation ability. This study demonstrates the feasibility of a salt-responsive bactericidal release surface; however, the high salt concentration required may limit its application. To address this issue, Wu *et al.* selected a conductive substrate material and used an electric field to aid the responsive release of polyurethane brushes at low salt concentrations (~0.12 mol/L) (Fig. S4E in Supporting information) [181]. With the assistance of an electric field, anions migrate and accumulate on the surface of the material, causing local high salt concentration ions, which in turn trigger conformational changes in the polymer brush and release the attached bacteria (>93.0%). Therefore, using applied stimuli such as electric fields, magnetic fields, and ultrasound to assist in releasing dead bacteria may be a future research direction.

5. Summary and outlook

In the past few decades, researchers have become increasingly interested in AMPs, leading to explosive growth in the research and development of polymers. This review describes the antimicrobial properties and mechanisms of action of polymers in the perspective of wetting properties. It specifically summarizes the advantages of AMPs with different wettabilities under different application scenarios and explores the potential application fields of these materials (Table S1 in Supporting information). Hydrophilic AMPs are ideal for applications involving water-based environments or biological fluids, such as biomedical implants, marine antifouling coatings, and diagnostic devices [23,30,33]. Hydrophobic AMPs are used for water repellency and preventing wetting in applications such as self-cleaning coatings, food packaging, and water-repellent textiles [72,73]. Amphiphilic antibacterial polymers combine the advantages of hydrophilic and hydrophobic AMPs and balance hydrophilicity and hydrophobicity. With a deeper understanding of the antimicrobial mechanisms, amphiphilic polymers have been used in research on antimicrobial materials/coatings. One of the current trends in the development of AMPs is the selection of antimicrobial materials/surfaces with different wettabilities to meet the application requirements in different scenarios. Although AMPs have been rapidly developed over the past few years, further research is necessary for the practical and scale-up application of AMPs in daily life, as issues such as on-demand design, drug resistance, long-term activity, antimicrobial evaluation methods, and mass production still need to be systematically studied. Even though, some guidelines for the design of antimicrobial polymers soon become gradually clear according to the above previous research works.

(1) Both hydrophilic and hydrophobic AMPs have their appropriate performances for different application scenarios. Generally, hydrophilic polymers exhibit excellent efficacy for bacteria and hydrophobic polymers for fungi. Some responsive nanoagents based on amphiphilic polymers successfully integrate the antimicrobial and anti-adhesive properties *via* dynamic triggers or switches for complete microbial elimination. Besides, some specific environments are extremely complicated with bacteria, fungi, and mucedine. Therefore, the structure, interface, and surface properties of AMPs should be specifically designed according to the real application conditions, and a combined strategy is also an optimal option.
(2) As the antimolding ability of polymers in humid environments is crucial and it is quietly different from bacteria, the traditional antimicrobial polymers mediated by killing and damaging properties fail. To solve these situations, novel AMPs based on stereochemical design have been systematically verified against fungi (*A. niger, A. flavus, Mucor racemose, P. chrysogenum,* and *yeast*). More importantly, in introduction of chiral molecules on the surface of the polymer enables the anti-adhesion effect, which could guarantee the long-term maintenance of a clear interface. Thus, the stereochemical antimicrobial strategy is promising to design and develop new antimolding and anti-adhesion materials and surfaces for wide biomedical applications.
(3) In the clinic, medical devices are prohibited from adding nanometal agents, antibacterial agent dissolution, and membrane-damaging sterilization. Meanwhile, bactericidal polymer composites may increase the risk of drug resistance due to the multi-componnets [182]. Therefore, the design of antimicrobial performances born from intrinsic polymer itself rather than in combination with active agents counts most in real application scenarios. Furthermore, the design of AMPs can consider and obey the sensing and distinguishing characterization of mi-

croorganisms. Namely, microorganisms will actively depart once they distinguish a specifically prepared surface from the functionalized group information, like a chiral molecule, which will effectively avoid drug resistance.

(4) Finally, most AMPs exhibit excellent antimicrobial stability under laboratory conditions but do not evaluate their efficiency in practical applications. Meanwhile, how to ensure the quality and performance of batch products under scale-up production is still a burning question. More efforts should focus on performance optimization for specific situations. In addition, most AMPs/surfaces are prepared using expensive methods, which makes the scaled-up process challenging. Therefore, reducing the production cost or using AMPs as coating is an issue that must be considered in the near future.

Last but not least, challenges and opportunities coexist. All the problems right now will bring about the technology development. Therefore, we believe that AMPs will be increasingly used in real-life products and devices, and this up-and-coming class of materials will protect human health worldwide.

Declaration of competing interest

The authors declare that they have no known competing financial interests or personal relationships that could have appeared to influence the work reported in this paper.

Acknowledgment

This work was supported by the National Natural Science Foundation of China (Nos. 52273118, 22275013).

Supplementary materials

Supplementary material associated with this article can be found, in the online version, at doi:10.1016/j.cclet.2024.109768.

References

[1] J.F.W. Chan, S. Yuan, K.H. Kok, et al., Lancet 395 (2020) 514–523.
[2] K. Sun, Z. Ding, X.Y. Jia, et al., CCS Chem. 6 (2024) 487–496.
[3] L. Liu, Y. Deng, S. Xia, et al., BMC Infect. Dis. 23 (2023) 589.
[4] C. Sohrabi, Z. Alsafi, N. O'Neill, et al., Int. J. Surg. 76 (2020) 71–76.
[5] K. Xue, C.H. Yang, C. Wang, et al., CCS Chem. 4 (2021) 272–285.
[6] P. Yuan, X. Ding, Y.Y. Yang, Q.H. Xu, Adv. Healthc. Mater. 7 (2018) 1701392.
[7] J. Abraham, K. Dowling, S. Florentine, Materials 14 (2021) 3444.
[8] R. Emmanuel, S. Palanisamy, S.M. Chen, et al., Mater. Sci. Eng. C 56 (2015) 374–379.
[9] S.W.X. Ong, Y.K. Tan, P.Y. Chia, et al., JAMA 323 (2020) 1610–1612.
[10] G. Kampf, Infect. Prev. Pract. 2 (2020) 100044.
[11] E. Maikranz, C. Spengler, N. Thewes, et al., Nanoscale 12 (2020) 19267–19275.
[12] R. Suman, M. Javaid, A. Haleem, et al., J. Clin. Exp. Hepatol. 10 (2020) 386–390.
[13] Y. Zhang, J. Lu, J. Wu, J. Wang, Y. Luo, Ecotoxicol. Environ. Saf. 187 (2020) 109852.
[14] L.M. Stabryla, K.A. Johnston, N.A. Diemler, et al., Nat. Nanotechnol. 16 (2021) 996–1003.
[15] X. Wang, Y.Q. Wang, D.C. Wu, Chin. J. Polym. Sci. 41 (2023) 564–573.
[16] B. Li, T.J. Webster, J. Orthop. Res. 36 (2018) 22–32.
[17] M. Serra-Burriel, M. Keys, C. Campillo-Artero, et al., PLoS One 15 (2020) e0227139.
[18] Z.H. Yu, X. Li, F. Xu, et al., Angew. Chem. Int. Ed. 59 (2020) 3658–3664.
[19] H. Mohanty, S. Pachpute, R.P. Yadav, Folia. Microbiol. 66 (2021) 727–739.
[20] C. Wu, J. Lu, L. Ruan, J. Yao, Infect. Drug Resist. 16 (2023) 1499–1509.
[21] D. Pranantyo, K. Zhang, Z. Si, Z. Hou, M.B. Chan-Park, Biomacromolecules 23 (2022) 1873–1891.
[22] Y. Wu, K. Chen, J. Wang, et al., Prog. Polym. Sci. 141 (2023) 101679.
[23] P. Pham, S. Oliver, C. Boyer, Macromol. Chem. Phys. 224 (2023) 2200226.
[24] H. Takahashi, I. Sovadinova, K. Yasuhara, et al., WIREs Nanomed. Nanobiotechnol. 15 (2023) e1866.
[25] L.P. Datta, R. Mukherjee, S. Biswas, T.K. Das, Langmuir 33 (2017) 14195–14208.
[26] A. Khlyustova, M. Kirsch, X. Ma, Y. Cheng, R. Yang, J. Mater. Chem. B 10 (2022) 2728–2739.
[27] F. Wang, B. Wang, X. Li, et al., Prog. Org. Coat. 142 (2020) 105576.
[28] R. Cuervo-Rodríguez, F. López-Fabal, A. Muñoz-Bonilla, M. Fernández-García, Materials 14 (2021) 7477.
[29] S. Pourhashem, A. Seif, F. Saba, et al., J. Mater. Sci. Technol. 118 (2022) 73–113.
[30] Q. Xu, L. Ying, X. Wang, Y.Y. Zhang, P. Wang, Fibers Polym. 23 (2022) 944–953.
[31] C. Wang, P. Makvandi, E.N. Zare, F.R. Tay, L. Niu, Adv. Ther. 3 (2020) 2000024.
[32] X. Wu, J. Wu, C. Mu, C. Wang, W. Lin, Ind. Eng. Chem. Res. 60 (2021) 15004–15018.
[33] T. Wei, Y. Qu, Y. Zou, Y. Zhang, Q. Yu, Curr. Opin. Chem. Eng. 34 (2021) 100727.
[34] H. Luo, X.Q. Yin, P.F. Tan, et al., J. Mater. Chem. B 9 (2021) 2802–2815.
[35] Q. Borjihan, A. Dong, Biomater. Sci. 8 (2020) 6867–6882.
[36] Y. Yang, Z. Cai, Z. Huang, X. Tang, X. Zhang, Polym. J. 50 (2018) 33–44.
[37] Z. Chen, Z. Lv, Y. Sun, Z. Chi, G. Qing, J. Mater. Chem. B 8 (2020) 2951–2973.
[38] X. Ding, A. Wang, W. Tong, F.J. Xu, Small 15 (2019) 1900999.
[39] X. Xu, X. Huang, Y. Chang, et al., Biomacromolecules 22 (2021) 330–339.
[40] Z. Tong, H. Guo, Z. Di, et al., Colloids Surf. B 213 (2022) 112392.
[41] X. Yang, P. Huang, H. Wang, et al., Colloids Surf. B 160 (2017) 136–143.
[42] G. Sathishkumar, K. Gopinath, K. Zhang, et al., J. Mater. Chem. B 10 (2022) 2296–2315.
[43] Y.C. Chiang, Y. Chang, A. Higuchi, W.Y. Chen, R.C. Ruaan, J. Memb. Sci. 339 (2009) 151–159.
[44] Y.P. Tang, T. Cai, D. Loh, G.S. O'Brien, T.S. Chung, Sep. Purif. Technol. 176 (2017) 294–305.
[45] J.S. Chen, Y.S. Ting, H.M. Tsou, T.Y. Liu, Surf. Coat. Technol. 344 (2018) 621–625.
[46] D. Li, Q. Wei, C. Wu, et al., Adv. Colloid Interface Sci. 278 (2020) 102141.
[47] J. Ennis, L. Sjöström, T. Åkesson, B. Jönsson, Langmuir 16 (2000) 7116–7125.
[48] A.A. D'souza, R. Shegokar, Expert Opin. Drug Deliv. 13 (2016) 1257–1275.
[49] E. Ostuni, R.G. Chapman, R.E. Holmlin, S. Takayama, G.M. Whitesides, Langmuir 17 (2001) 5605–5620.
[50] K.D. Park, Y.S. Kim, D.K. Han, et al., Biomaterials 19 (1998) 851–859.
[51] L. Peng, L. Chang, X. Liu, et al., ACS Appl. Mater. Interfaces 9 (2017) 17688–17692.
[52] R. Wanka, F. Koschitzki, V. Puzovic, et al., ACS Appl. Mater. Interfaces 13 (2021) 6659–6669.
[53] L.L. Guo, Y.F. Cheng, X. Ren, et al., Colloids Surf. B 200 (2021) 111592.
[54] S. Kim, T. Gim, S.M. Kang, ACS Appl. Mater. Interfaces 7 (2015) 6412–6416.
[55] L. Peng, L. Chang, M. Si, et al., ACS Appl. Mater. Interfaces 12 (2020) 9718–9725.
[56] L. Mi, S. Jiang, Angew. Chem. Int. Ed. 53 (2014) 1746–1754.
[57] A. Laschewsky, Polymers 6 (2014) 1544–1601.
[58] Z. Chen, Langmuir 38 (2022) 4483–4489.
[59] P. Liu, G. Xu, D. Pranantyo, et al., ACS Biomater. Sci. Eng. 4 (2018) 40–46.
[60] G. Cheng, Z. Zhang, S. Chen, J.D. Bryers, S. Jiang, Biomaterials 28 (2007) 4192–4199.
[61] J.B. Schlenoff, Langmuir 30 (2014) 9625–9636.
[62] L. Zheng, H.S. Sundaram, Z. Wei, C. Li, Z. Yuan, React. Funct. Polym. 118 (2017) 51–61.
[63] G. Cheng, G. Li, H. Xue, et al., Biomaterials 30 (2009) 5234–5240.
[64] H.S. Sundaram, X. Han, A.K. Nowinski, et al., Adv. Mater. Interfaces 1 (2014) 1400071.
[65] Y. Kim, L.T. Thuy, Y. Kim, et al., Langmuir 38 (2022) 1550–1559.
[66] P. Sae-ung, A. Wijitamornloet, Y. Iwasaki, P. Thanyasrisung, V.P. Hoven, Macromol. Mater. Eng. 304 (2019) 1970022.
[67] B. Ran, C. Jing, C. Yang, X. Li, Y. Li, Appl. Surf. Sci. 450 (2018) 77–84.
[68] Q. Liu, W. Li, H. Wang, et al., Langmuir 32 (2016) 7866–7874.
[69] J. Wang, L. Wang, C. Wu, et al., ACS Appl. Mater. Interfaces 12 (2020) 46816–46826.
[70] X. Yang, J. Hou, Y. Tian, et al., Sci. China Technol. Sci. 65 (2022) 1000–1010.
[71] R. Li, Z. Wang, X. Lian, X. Hu, Y. Wang, CCS Chem. 2 (2020) 245–256.
[72] S. Wang, J. Li, Y. Cao, et al., Adv. Fiber Mater. 4 (2021) 119–128.
[73] M. Haktaniyan, M. Bradley, Chem. Soc. Rev. 51 (2022) 8584–8611.
[74] Z. Si, W. Zheng, D. Prananty, et al., Chem. Sci. 13 (2022) 345–364.
[75] S. Zhang, X. Yang, B. Tang, et al., Chem. Eng. J. 336 (2018) 123–132.
[76] X. Fu, Y. Zhang, X. Jia, Y. Wang, T. Chen, Molecules 27 (2022) 1267.
[77] Y. Dong, L. Liu, J. Sun, et al., J. Mater. Chem. B 9 (2021) 8321–8329.
[78] S. Bai, X. Li, Y. Zhao, L. Ren, X. Yuan, ACS Appl. Mater. Interfaces 12 (2020) 12305–12316.
[79] H. Zhang, T. Fang, X. Yao, Y. Xiong, W. Zhu, Chem. Eng. J. 440 (2022) 135949.
[80] D. Wei, Q. Ma, Y. Guan, et al., Mater. Sci. Eng. C 29 (2009) 1776–1780.
[81] Q. Lin, L. Wu, W. Hu, et al., Surf. Interfaces 29 (2022) 101708.
[82] M.E. Villanueva, J.A. González, E. Rodríguez-Castellón, S. Teves, G.J. Copello, Mater. Sci. Eng. C 67 (2016) 214–220.
[83] W. Cao, D. Wei, A. Zheng, Y. Guan, Eur. Polym. J. 118 (2019) 231–238.
[84] A. Dong, Y.J. Wang, Y. Gao, T. Gao, G. Gao, Chem. Rev. 117 (2017) 4806–4862.
[85] H.W. Chien, T.H. Chiu, Y.L. Lee, Langmuir 37 (2021) 8037–8044.
[86] Z. Jing, K. Xiu, X. Ren, Y. Sun, Colloids Surf. B 166 (2018) 210–217.
[87] F. Wang, M. Liu, R. Ding, et al., ACS Appl. Bio Mater. 2 (2019) 3668–3677.
[88] J. Tan, Y. Zhao, J.L. Hedrick, Y.Y. Yang, Adv. Healthc. Mater. 11 (2022) 2100482.
[89] A.C. Engler, J.P.K. Tan, Z.Y. Ong, et al., Biomacromolecules 14 (2013) 4331–4339.
[90] L. Wang, X. Guo, H. Zhang, et al., Coatings 12 (2022) 1469.
[91] Y. Zhan, S. Yu, A. Amirfazli, A.R. Siddiqui, W. Li, Adv. Eng. Mater. 24 (2022) 2101053.
[92] X. Yao, Y. Song, L. Jiang, Adv. Mater. 23 (2011) 719–734.
[93] D. Zhang, Z. Liu, G. Wu, et al., ACS Appl. Bio Mater. 4 (2021) 6351–6360.
[94] N. Keller, J. Bruchmann, T. Sollich, et al., ACS Appl. Mater. Interfaces 11 (2019) 4480–4487.
[95] P.C. Wang, D. Lu, H. Wang, R.K. Bai, Polymers 11 (2019) 1440.

[96] Z. Qiao, D. Xu, Y. Yao, et al., Polym. Int. 68 (2019) 1361–1366.
[97] Y. Zhang, Y.H. Qi, Z.P. Zhang, G.Y. Sun, J. Coat. Technol. Res. 12 (2015) 215–223.
[98] Q. Zeng, H. Zhou, J. Huang, Z. Guo, Nanoscale 13 (2021) 11734–11764.
[99] A.M.C. Maan, A.H. Hofman, W.M. de Vos, M. Kamperman, Adv. Funct. Mater. 30 (2020) 2000936.
[100] J. Li, T. Kleintschek, A. Rieder, et al., ACS Appl. Mater. Interfaces 5 (2013) 6704–6711.
[101] L. Xiao, J. Li, S. Mieszkin, et al., ACS Appl. Mater. Interfaces 5 (2013) 10074–10080.
[102] Y. Bi, Z. Wang, L. Lu, et al., Prog. Org. Coat. 133 (2019) 387–394.
[103] Q. Bao, N. Nishimura, H. Kamata, et al., Colloids Surf. B 151 (2017) 363–371.
[104] I. Laitman, M. Natan, E. Banin, S. Margel, Colloids Surf. B 115 (2014) 8–14.
[105] P. Zhu, W. Meng, Y. Huang, RSC Adv. 7 (2017) 3179–3189.
[106] X. Wang, H. Gan, T. Sun, et al., Soft Matter 6 (2010) 3851–3855.
[107] A.L. Hook, C.Y. Chang, J. Yang, et al., Nat. Biotechnol. 30 (2012) 868–875.
[108] L. Luo, G. Li, D. Luan, et al., ACS Appl. Mater. Interfaces 6 (2014) 19371–19377.
[109] J. Xu, H. Zhao, Z. Xie, et al., Adv. Healthc. Mater. 8 (2019) 1–10.
[110] X. Sun, Z. Qian, L. Luo, et al., ACS Appl. Mater. Interfaces 8 (2016) 28522–28528.
[111] X. Wang, S. Jing, Y. Liu, S. Liu, Y. Tan, Polymer 116 (2017) 314–323.
[112] Q. Cheng, Y.Y. Peng, A.B. Asha, et al., Biomater. Sci. 10 (2022) 1787–1794.
[113] J. Wu, C. Wang, C. Mu, W. Lin, Eur. Polym. J. 108 (2018) 498–506.
[114] J. Xu, Z. Xie, F. Du, X. Wang, J. Mater. Sci. Technol. 69 (2021) 79–88.
[115] X. Li, Z. Xie, G. Li, et al., ACS Appl. Polym. Mater. 3 (2021) 3702–3707.
[116] J. Li, P. Zhang, M. Yang, et al., ACS Appl. Polym. Mater. 4 (2022) 1922–1930.
[117] P. Zhang, M. Yang, J. Li, et al., Colloid Interface Sci. Commun. 46 (2022) 100567.
[118] P. Zhang, J. Li, M. Yang, et al., ACS Biomater. Sci. Eng. 8 (2021) 570–578.
[119] F. Song, L. Zhang, R. Chen, et al., ACS Appl. Mater. Interfaces 13 (2021) 33417–33426.
[120] C. Chen, Z. Xie, P. Zhang, Y. Liu, X. Wang, Colloid Interface Sci. Commun. 40 (2021) 100336.
[121] P. Zhang, X. Chen, F. Bu, et al., ACS Appl. Mater. Interfaces 15 (2023) 9926–9939.
[122] K. Yang, J. Shi, L. Wang, et al., J. Mater. Sci. Technol. 99 (2022) 82–100.
[123] R. An, Y. Dong, J. Zhu, C. Rao, Colloids Surf. B 159 (2017) 108–117.
[124] S. Mo, B. Mehrjou, K. Tang, et al., Chem. Eng. J. 392 (2020) 123736.
[125] C.M. Magin, S.P. Cooper, A.B. Brennan, Mater. Today 13 (2010) 36–44.
[126] L. Huang, C.J. Liu, Supramol. Mater. 1 (2022) 100008.
[127] L.M. Ward, R.M. Shah, J.D. Schiffman, S.T. Weinman, ACS EST Water 2 (2022) 1593–1601.
[128] S.V. Oopath, A. Baji, M. Abtahi, et al., Adv. Mater. Interfaces 10 (2023) 2201425.
[129] M. Yang, Y. Ding, X. Ge, Y. Leng, Colloids Surf. B 135 (2015) 549–555.
[130] R. Vasudevan, A.J. Kennedy, M. Merritt, F.H. Crocker, R.H. Baney, Colloids Surf. B 117 (2014) 225–232.
[131] G. Tullii, S. Donini, C. Bossio, et al., ACS Appl. Mater. Interfaces 12 (2020) 5437–5446.
[132] K. Glinel, P. Thebault, V. Humblot, C.M. Pradier, T. Jouenne, Acta Biomater. 8 (2012) 1670–1684.
[133] J. Hasan, K. Chatterjee, Nanoscale 7 (2015) 15568–15575.
[134] Z. Liu, Y. Yi, L. Song, et al., Acta Biomater. 141 (2022) 198–208.
[135] A. Tripathy, P. Sen, B. Su, W.H. Briscoe, Adv. Colloid Interface Sci. 248 (2017) 85–104.
[136] K.K. Chung, J.F. Schumacher, E.M. Sampson, et al., Biointerphases 2 (2007) 89–94.
[137] S.T. Reddy, K.K. Chung, C.J. McDaniel, et al., J. Endourol. 25 (2011) 1547–1552.
[138] H.W. Chien, X.Y. Chen, W.P. Tsai, M. Lee, Colloids Surf. B 186 (2020) 110738.
[139] A. Braem, L. Van Mellaert, T. Mattheys, et al., J. Biomed. Mater. Res. A 102 (2014) 215–224.
[140] Y. Cheng, G. Feng, C.I. Moraru, Front. Microbiol. 10 (2019) 410243.
[141] D.P. Linklater, S. Saita, T. Murata, et al., ACS Appl. Nano Mater. 5 (2022) 2578–2591.
[142] A. Tripathy, S. Pahal, R.J. Mudakavi, et al., Biomacromolecules 19 (2018) 1340–1346.
[143] R. Fontelo, D. Soares da Costa, R.L. Reis, R. Novoa-Carballal, I. Pashkuleva, Acta Biomater. 112 (2020) 174–181.
[144] S. He, M. Hou, S. Shan, et al., React. Funct. Polym. 183 (2023) 105495.
[145] E.F. Palermo, K. Lienkamp, E.R. Gillies, P.J. Ragogna, Angew. Chem. 131 (2019) 3728–3731.
[146] M.A. Rahman, M. Bam, E. Luat, et al., Nat. Commun. 9 (2018) 5231.
[147] P. Pham, S. Oliver, E.H.H. Wong, C. Boyer, Polym. Chem. 12 (2021) 5689–5703.
[148] X. Liao, K. Niu, F. Liu, et al., Molecules 27 (2022) 5059.
[149] C. Wang, J. Chen, J. Xu, J. Fu, A.C.S. Appl, Polym. Mater. 3 (2021) 3416–3427.
[150] T.F. dos Reis, P.A. de Castro, R.W. Bastos, et al., Nat. Commun. 14 (2023) 2052.
[151] S. Mankoci, J. Ewing, P. Dalai, et al., Biomacromolecules 20 (2019) 4096–4106.
[152] A. Sengupta, S. Kumar Ethirajan, M. Kamaz, M. Jebur, R. Wickramasinghe, Sep. Purif. Technol. 212 (2019) 307–315.
[153] A. Muñoz-Bonilla, M. Fernández-García, Eur. Polym. J. 105 (2018) 135–149.
[154] E.F. Palermo, K. Kuroda, Appl. Microbiol. Biotechnol. 87 (2010) 1605–1615.
[155] C. Peng, A. Vishwakarma, S. Mankoci, H.A. Barton, A. Joy, Biomacromolecules 20 (2019) 1675–1682.
[156] R. Bhat, L.L. Foster, G. Rani, S. Vemparala, K. Kuroda, RSC Adv. 11 (2021) 22044–22056.
[157] H. Etayash, Y. Qian, D. Pletzer, et al., J. Med. Chem. 63 (2020) 12921–12928.
[158] X. Liu, Y. Yang, M. Han, et al., Adv. Healthc. Mater. 11 (2022) 2201091.
[159] Y. Qian, F. Qi, Q. Chen, et al., ACS Appl. Mater. Interfaces 10 (2018) 15395–15400.
[160] Q. Gao, X. Li, W. Yu, et al., ACS Appl. Mater. Interfaces 12 (2020) 2999–3010.
[161] Z. Lu, Y. Wu, Z. Cong, et al., Bioact. Mater. 6 (2021) 4531–4541.
[162] A. Vishwakarma, F. Dang, A. Ferrell, H.A. Barton, A. Joy, J. Am. Chem. Soc. 143 (2021) 9440–9449.
[163] A.M. Curreri, S. Mitragotri, E.E.L. Tanner, Adv. Sci. 8 (2021) 2004819.
[164] J. Guo, Q. Xu, Z. Zheng, et al., ACS Macro. Lett. 4 (2015) 1094–1098.
[165] J. Qin, J. Guo, Q. Xu, et al., ACS Appl. Mater. Interfaces 9 (2017) 10504–10511.
[166] X. Liu, L. Chang, L. Peng, et al., ACS Appl. Mater. Interfaces 13 (2021) 48358–48364.
[167] W. Liu, Y. Dong, S. Liu, et al., Macromol. Rapid Commun. 40 (2019) 1900379.
[168] M. Ghasemlou, F. Daver, E.P. Ivanova, J.W. Rhim, B. Adhikari, ACS Appl. Mater. Interfaces 11 (2019) 22897–22914.
[169] T. Wei, W. Zhan, Q. Yu, H. Chen, ACS Appl. Mater. Interfaces 9 (2017) 25767–25774.
[170] W. Zhan, T. Wei, L. Cao, et al., ACS Appl. Mater. Interfaces 9 (2017) 3505–3513.
[171] Y. Wang, J. Wu, D. Zhang, et al., J. Mater. Chem. B 7 (2019) 5762–5774.
[172] Q. Yu, Z. Wu, H. Chen, Acta Biomater. 16 (2015) 1–13.
[173] H. Yang, G. Li, J.W. Stansbury, et al., ACS Appl. Mater. Interfaces 8 (2016) 28047–28054.
[174] H. Chen, J. Yang, S. Xiao, et al., Acta Biomater. 40 (2016) 62–69.
[175] Y. Lu, Y. Wu, J. Liang, M.R. Libera, S.A. Sukhishvili, Biomaterials 45 (2015) 64–71.
[176] S. Yan, H. Shi, L. Song, et al., ACS Appl. Mater. Interfaces 8 (2016) 24471–24481.
[177] G. Xu, K.G. Neoh, E.T. Kang, S.L.M. Teo, ACS Sustain. Chem. Eng. 8 (2020) 2586–2595.
[178] Q. Yu, J. Cho, P. Shivapooja, L.K. Ista, G.P. López, ACS Appl. Mater. Interfaces 5 (2013) 9295–9304.
[179] Q. Yu, L.K. Ista, G.P. López, Nanoscale 6 (2014) 4750–4757.
[180] Y. Fu, Y. Wang, L. Huang, et al., Ind. Eng. Chem. Res. 57 (2018) 8938–8945.
[181] J. Wu, D. Zhang, Y. Wang, et al., Langmuir 35 (2019) 8285–8293.
[182] A. Panáček, L. Kvítek, M. Smékalová, et al., Nat. Nanotechnol. 13 (2018) 65–71.